Determination of Structural Fragility Curves of Various Building Types for Seismic Vulnerability Assessment in the Sarpol-e Zahab City

Fereshteh Izanloo[1] and Aliakbar Yahyaabadi[2*]*

1. Faculty of Engineering, University of Bojnord, Bojnord, Iran
2. Assistant Professor, University of Bojnord, Bojnord, Iran,
* Corresponding Author; email: A.yahyaabadi@ub.ac.ir

Received: 26/08/2018
Accepted: 05/11/2018

ABSTRACT

Seismic vulnerability assessment helps to estimate the extent and the probability of damage to buildings due to the potential earthquake hazard. Determination of structural fragility curves of buildings is one of the most important steps in seismic vulnerability assessment. The fragility curve predicts the probability of exceeding specific damage states for a seismic intensity parameter. This paper is focused on the development of structural fragility curves for different building types in the Sarpol-e Zahab city. For this purpose, a reconnaissance survey was conducted after the Sarpol-e Zahab earthquake of November 12, 2017 to identify the damage state of various buildings based on the HAZUS Methodology. Then, the improved-displacement coefficient method implemented in the SELENA software was used for expressing building loss probabilities. In order to find out which level of the seismic design can be used in defining the fragility curves, different weights were considered to apply to the HAZUS fragility curves of high, moderate, low and pre-code to be used in the logic tree method. Finally, the mean and standard deviation values were introduced for the construction of fragility curves with the lognormal distribution for the seven Iranian building types.

Keywords:
Structural fragility curves; Seismic vulnerability assessment; Damage state; Building types; Sarpol-e Zahab 2017 earthquake

1. Introduction

Seismic vulnerability assessment of buildings in urban areas is one of the priorities of crisis management institutions for planning to reduce risks in the future. The results of the vulnerability assessment are influenced by several factors including the analysis method and the data needed to perform the analysis through the selected method such as fragility curves and attenuation relations. There is an intense interest in developing seismic vulnerability assessment models that are able to generate reliable damage scenarios to support the decision-making process in disaster prevention and crisis management policies. In using the improved-displacement coefficient method, the most influencing parameters in vulnerability assessment are the selection of the fragility curves for the buildings and the seismic hazard model adopted in the analysis.

Various methods have the capability to assess seismic vulnerability. For example, in 2016, Kumar et al. [1] present an approach on how to conduct Rapid Visual Screening (RVS) for five types of buildings in Himachal Pradesh state. They have calculated the RVS scores for 9099 buildings and plotted the normal distribution curves for each building type to understand the

distribution of buildings in this state. Finally, a new modified format for performing RVS has been proposed at the end.

Development of appropriate fragility curves is the matter of concern in various studies. Del Gaudio et al. [2] proposed the fragility curves for RC buildings using a database of 7597 private buildings after the L'Aquila 2009 earthquake in 2016. For this purpose, damage grades were derived from damage data to single building components according to the European Macro Seismic scale EMS-98. They also compared the suggested fragility curves with the main empirical fragility curves for RC buildings from literature studies.

In another study, observational data collected in the L'Aquila 2009 earthquake was compared with a predicted damage scenario. A simplified analytical method was used for seismic vulnerability assessment of reinforced concrete buildings at large scale [3].

In 2016, Toma-Danila [4] studied on the possible seismic damage of residential buildings in Bucharest, Romania, at neighborhood resolution. They used the improved displacement coefficient analytical method to compute damage probabilities based on the 48 vulnerability curves for buildings included in the SELENA software. The intensity of earthquake ground motion was determined using deterministic seismic hazard scenarios including the maximum possible earthquake.

The first study on seismic fragility curves in Iran was carried out by Tavakoli and Tavakoli [5] in 1993 based on the Manjil-Rudbar earthquake data in 1990, regardless of the importance of construction year, seismic code, height, and type of structures. In 2000, the Japan International Cooperation Agency (JICA) [6] has developed the vulnerability curves for nine types of structures in Tehran using the ATC-13 method, Tavakoli and Tavakoli fragility curves and engineering judgment. Mostafaei and Kabeyasawa [7] earned damage rates to some of Bam's buildings using the Bam 2003 Earthquake Damage data.

Bakhshi and Karimi [8] by considering the cumulative absolute velocity as an intensity measure (IM), have conducted a study on the vulnerability assessment of reinforced and unreinforced masonry buildings in Iran. Jalalian [9] developed a PGA-based analytical fragility function for Tehran's masonry buildings in 2006. In 2013, Kazemi et al. [10] conducted the study on the effects of different strong ground motion records on fragility curves for Mashhad city in Iran. They defined structural limit states on each incremental dynamic analysis curve and estimated the corresponding damage measures.

In 2009, the fragility curve of a typical unreinforced brick masonry buildings was developed through a nonlinear analysis of the selected building in Tehran by Dare-Zereshki et al. [11]. In 2015, Sadeghi et al. [12] studied determining the vulnerability curves of 42 types of Iranian buildings. They used the logic-tree method to combine different curves by weighting in accordance with the condition of seismic code, construction provisions, and engineering judgment. In 2017, Kazemi et al. [13] determined fragility curves for steel braced frame structures using new spectral shape indicators and a weighted damage index. Their results show that the predicted median structural capacities are strongly influenced by spectral shape indicators.

Considering that damage and loss data from actual earthquakes can contribute to improvements of the vulnerability assessment methods, this study was focused on the development of fragility curves for various building types with respect to the realistic results observed after the Sarpol-e Zahab 2017 earthquake. To identify the real damage scenario, 200 buildings of different types were surveyed in various neighborhoods of the city. The HAZUS methodology was used to determine the structural damage state of each building [14]. Considering the collected damage data, we studied the possibility of using the fragility curves proposed by HAZUS in vulnerability assessment of the Sarpol-e Zahab city. The aim of this study is to determine which level of the seismic design can be used in defining the fragility curves for various building types according to the HAZUS approach. This study proposed the weights to apply to the HAZUS fragility curves of high, moderate, low and pre-code to be used in the logic tree method in the vulnerability assessment procedure.

2. Real Damage Scenario

The collected information includes the geographical location of the building, the address, the

number of floors, the year of construction, building area with precision square meters, the type of the structure and the damage state. According to the HAZUS approach, damage states are categorized into four ranges: slight, moderate, extensive and complete. For example, the moderate damage state ranges from the threshold of the moderate damage up to the threshold of the extensive damage. General descriptions of the four structural damage states for various building types are provided as the field survey form, adapted from reference [14], in Figure (1).

Building Vulnerability Assessment Form

Name of the investigator:			**Data:**	
General information:				
Address: **GPS Coordinates:** Longitude: Latitude: **Average built-up area:**	**No. of occupants in the building:** Day:		Night:	
	Number of stories in the building: Unreinforced Masonry Bearing Walls :		1-2 ☐	3+ ☐
	Other buildings:	1-3 ☐	4-7 ☐	8+ ☐
	Design year: -1991 ☐	1991-2005 ☐	2005-2014 ☐	2014+ ☐
	Construction Year: -1991 ☐	1991-2005 ☐	2005-2014 ☐	2014+ ☐
Occupancy of use: RES1 ☐	RES3A ☐	RES3B ☐	RES3C ☐	RES3E ☐
Type of building structure: Steel Moment Frame ☐	Steel Braced Frame ☐		Concrete Shear Walls ☐	
Reinforced Concrete Moment Resisting Frames ☐	Unreinforced Masonry Bearing Walls ☐			

General descriptions of damage states:

Model building type:

	Steel Moment Frame (S1)		**Steel Braced Frame (S2)**
Slight ☐	Minor deformations in connections hairline cracks in few welds	**Slight** ☐	**Few steel braces have yielded** minor stretching and/or buckling of slender brace member minor cracks in welded connections minor deformations in bolted brace connections
Moderate ☐	Some steel members have yielded permanent rotations at connections few welded connections may exhibit major cracks through welds few bolted connections may exhibit broken bolts enlarged bolt holes	**Moderate** ☐	**Some steel braces have yielded** stretching and/or buckling of braces buckled braces, cracked welds, failed bolted connections
Extensive ☐	**Most steel members have exceeded their yield capacity** significant permanent lateral deformation of the structure **Some of the structural members or connections may have exceeded their ultimate capacity** major permanent member rotations at connections buckled flanges failed connections Partial collapse of portions of structure is possible	**Extensive** ☐	**Most steel brace and other members have exceeded their yield capacity** significant permanent lateral deformation of the structure **Some structural members or connections have exceeded their ultimate capacity** buckled or broken braces flange buckling, broken welds, or failed bolted connections Anchor bolts at columns may be stretched Partial collapse of portions of structure is possible
Complete ☐	**Significant portion of the structural elements have exceeded their ultimate capacities** some critical structural elements or connections have failed dangerous permanent lateral displacement partial collapse or collapse of the building	**Complete** ☐	**Most the structural elements have reached their ultimate capacities** some critical members or connections have failed dangerous permanent lateral deflection partial collapse or collapse of the building

Figure 1. Building vulnerability assessment form used for surveying (adapted from reference [14]).

General descriptions of damage states continued:

Model building type:

Reinforced Concrete Moment Resisting Frames (C1)			**Concrete Shear Walls (C2)**		
Slight	☐	Flexural or shear type hairline cracks in some beams and columns near joints or within joints	**Slight**	☐	Diagonal hairline cracks on most concrete shear wall surfaces minor concrete spalling at few locations
Moderate	☐	Most beams and columns exhibit hairline cracks **some of the frame elements have reached yield capacity** Larger flexural cracks and some concrete spalling.	**Moderate**	☐	Most shear wall surfaces exhibit diagonal cracks **some shear walls have exceeded yield capacity** larger diagonal cracks and concrete spalling at wall ends
Extensive	☐	**Some of the frame elements have reached their ultimate capacity** large flexural cracks, spalled concrete and buckled main reinforcement	**Extensive**	☐	**Most concrete shear walls have exceeded their yield capacities** **some walls have exceeded their ultimate capacities** large, through-the-wall diagonal cracks extensive spalling around the cracks visibly buckled wall reinforcement rotation of narrow walls with inadequate foundations Partial collapse may occur due to failure of nonductile columns
Complete	☐	Structure is collapsed or in imminent danger of collapse			
Unreinforced Masonry Bearing Walls (URM)			**Complete**	☐	Structure has collapsed in imminent danger of collapse due to failure of most of the shear walls and failure of some critical beams or columns.
Slight	☐	Diagonal, stair-step hairline cracks on masonry wall surfaces larger cracks around door and window openings in walls movements of lintels; cracks at the base of parapets	**Other building type**		
Moderate	☐	Most wall surfaces exhibit diagonal cracks some of the walls exhibit larger diagonal cracks masonry walls may have visible separation from diaphragms significant cracking of parapets some masonry may fall from walls or parapets	In the case of a building other than the one mentioned, its damage is described in this section:		
Extensive	☐	walls have suffered extensive cracking Some parapets and gable end walls have fallen Beams or trusses may have moved relative to their supports			
Complete	☐	Structure has collapsed in imminent danger of collapse due to in-plane or out-of-plane failure of the walls			

Figure 1. Continue.

Different types of the surveyed buildings are shown in Table (1). Overall, there are three main building types: concrete, steel, and masonry bearing wall and these can be further subdivided into seven classes according to the structural system and the building height as shown in the first column of Table (1). Figure (2) provides the area and the number of buildings surveyed for each of the seven building types. Besides, the area of the surveyed buildings in each district of Sarpol-e Zahab can be found in Table (2).

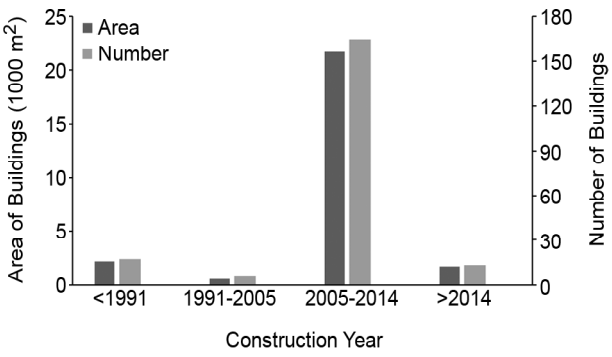

Figure 2. Area and number of surveyed buildings for various building types.

Table 1. Building types surveyed in Sarpol-e Zahab city.

Type	Structural System	Height
C1L	Concrete Moment Frame	Low-Rise (1-3)
C1M		Mid-Rise (4-7)
S1L	Steel Moment Frame	Low-Rise (1-3)
S1M		Mid-Rise (4-7)
S2L	Steel Braced Frame	Low-Rise (1-3)
S2M		Mid-Rise (4-7)
URML	Unreinforced Masonry Bearing Walls	Low-Rise (1-2)

Table 2. Area of surveyed buildings in each district.

Label	District	Area of Surveyed Buildings (sqr Meters)
1	Shahid Shiroodi Maskan-e Mehr	5220
2	Around the Shahid Shiroodi Maskan-e Mehr	2187
3	Alvand Maskan-e Mehr	4143
4	Around the Technical and Vocational Training Organization	2440
5	Fooladi Neighborhood	4556
6	Za'faran Neighborhood	2114
7	Ahmadabad Neighborhood	2781
8	Tarvij Sreet Neighborhood	2163
9	Shahrak-e Zerae Ghareblagh Neighborhood	600

The area and the number of surveyed buildings with the damage states Slight (S), Moderate (M), Extensive (E), and Complete (C) have been derived from the statistical elaboration of the surveyed data collected after the earthquake, shown in Figure (3). From this figure, it can be said that 28%, 35%, 23% and 14% of the surveyed buildings have experienced slight, moderate, extensive, and complete damage states, respectively. Damage scenario for each type of building is shown in Figure (4). This figure reveals that the observation of complete damage state is mainly related to unreinforced masonry buildings (URML) and low rise moment frames (C1L and S1L).

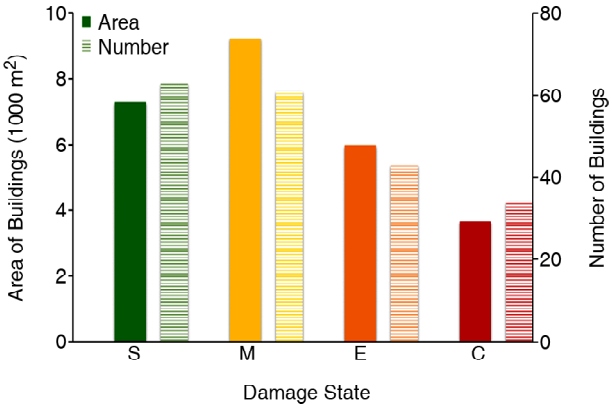

Figure 3. Observed damage scenario for all buildings.

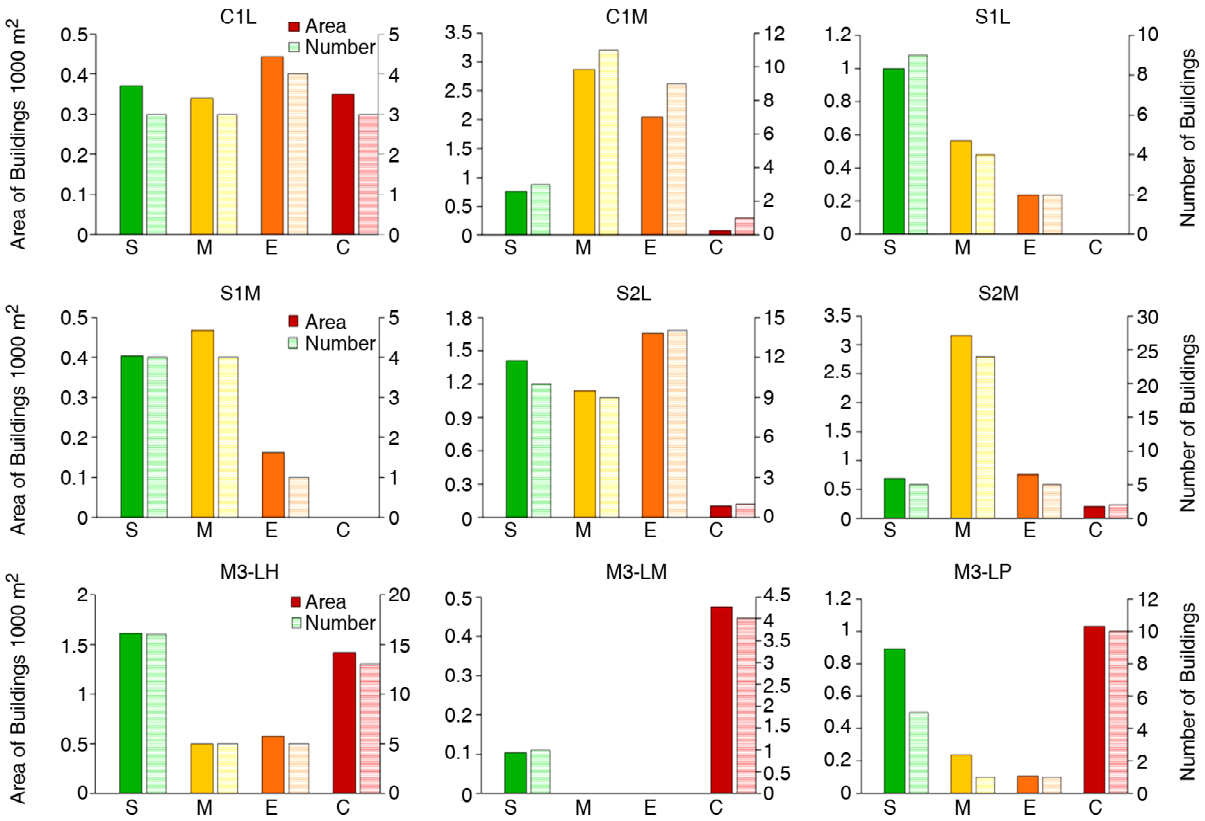

Figure 4. Observed damage scenario for all building types in the Sarpol-e Zahab city.

3. Analytical Damage Scenario

The objective is to statistically assess the seismic risk of areas at the territorial-administrative zone level, and not at a single building level. For this reason, a similar approach to HAZUS was used to estimate the physical damage in this study [15]. HAZUS approach is based on the analytical methods used for calculation of the building failure probability. These methods essentially involve the calculation of the "performance point" of a building used with fragility curves of a certain damage state to determine a damage probability. To estimate the performance point of buildings, the first method employed by an earthquake loss estimation software was the capacity-spectrum method. Since then, new improved methods were developed. One of them is the Improved-Displacement Coefficient Method (I-DCM). In I-DCM, the maximum nonlinear displacement demand of the building is estimated by multiplying the displacement demand of the equivalent SDOF by a series of coefficients [16].

This study used the SELENA open-source software to apply the I-DCM method. The overall process of achieving physical damage to buildings in Selena software is schematically presented in Figure (5). This figure implies that for deterministic seismic risk assessment, information about the earthquake, the attenuation relationships, the type of soil in each district and building inventory are required.

4. Earthquake Scenario

The parameters of Sarpol-e Zahab 2017 earthquake, obtained from Iranian Seismological Center report, are as follows: moment magnitude is equal to 7.3, focal depth is equal to 18 km, fault mechanism is reverse, and the latitude and longitude of the epicenter are 34.77° and 45.76°, respectively. The equation proposed by Earthquake Model of Middle East (EMME) used to calculate the surface wave magnitude [18].

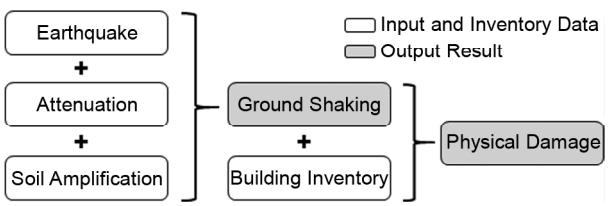

Figure 5. Principle flowchart of a deterministic analysis using the SELENA-tool [17].

5. Soil Type

The amplitude and frequency content of the surface seismic ground motion are dependent on the sedimentary soils on the site. According to the field observations and the report of International Institute of Earthquake Engineering and Seismology (IIEES) [19], the soil type for the various neighborhoods was assumed to be of type III, except for Ahmadabad and Tarvij street neighborhoods, which assumed to be of type II.

6. Attenuation Relationships

Considering that there is no real-time data comply with the center points of the defined geographical units, the reliable ground motion prediction equations were used to predict the displacement demand of the equivalent SDOF at different geo units. For this purpose, the six attention relationships proposed by the Iranian guidelines for seismic hazard analysis [20] were considered, shown in Table (3). The logic tree method was used to consider the uncertainty associated with the attenuation relationships. Table (4) provides the comparison between the spectral accelerations with 5% damping obtained from various GMPEs with those obtained from the ground motion recorded at the Sarpol-e Zahab station. This table provides a reliable insight into the identification of GMPEs that appropriately incorporated the effects of the source to target region of the dataset. It can be observed that the attenuation relationships proposed by Akkar and Bommer [21], Boore et al. [22-25], and Campbell and Bozorgnia [26] can predict the real data at the Sarpol-e Zahab station with the minimum error regarding other considered GMPEs.

Table 3. Empirical ground motion prediction equations.

Label	Author(s)
1	Akkar and Bommer [21]
2	Boore et al. [22-25]
3	Campbel and Bozorgnia – NGA [26]
4	Abrahamson and Silva – NGA [27]
5	Chiou and Young – NGA [28]
6	Boore and Atkinson – NGA [29]

Table 4. Comparison between the spectral accelerations (5% damping) of the ground motion recorded at the Sarpol-e Zahab station with those obtained from various GMPEs (in terms of g).

		Period (sec)						Average Error
		0.1	0.2	0.3	0.4	0.5	0.6	
	Sarpol-e Zahab Station	0.735	1.030	1.326	1.561	1.191	1.534	
GMPEs	Akkar and Bommer [21]	0.650	0.938	0.973	0.927	0.834	0.732	0.387
	Boore et al. [22-25]	0.786	1.023	1.095	1.024	0.952	0.845	0.292
	Campbel and Bozorgnia [26]	0.846	1.093	1.102	1.031	0.943	0.867	0.308
	Abrahamnson and Silva [27]	0.671	1.024	1.090	0.917	0.722	0.608	0.391
	Chiou and Young [28]	0.982	1.116	0.976	0.812	0.670	0.581	0.484
	Boore and Atkinson [29]	0.565	0.738	0.695	0.617	0.517	0.464	0.630

Table 5. Combinations of seismic design levels and construction quality levels when seismic design level assumed moderate and low.

Mode	Construction Quality	Seismic Design Level				
		-1991	1991-1999	1999-2005	2005-2014	2014+
		Pre-code	Low-code	Low-code	Moderate-code	Moderate-code
Mode 1	Ordinary	Pre	Low	Low	Moderate	Moderate
Mode 2	Inferior	Pre	Pre	Pre	Low	Low

Table 6. Combinations of seismic design levels and construction quality levels when seismic design level assumed high and moderate.

Mode	Construction Quality	Seismic Design Level				
		-1991	1991-1999	1999-2005	2005-2014	2014+
		Pre-code	Moderate-code	Moderate-code	High-code	High-code
Mode 3	Ordinary	Pre	Moderate	Moderate	High	High
Mode 4	Inferior	Pre	Low	Low	Moderate	Moderate

7. Defining the Various Fragility Curves to be Considered

Seismic performance of buildings during an earthquake depends on the various factors, including the building type, the building height, the seismic zone location, the seismic design level, and the construction quality. Accordingly, the HAZUS methodology provides building damage functions in four states of high, moderate, low and pre-code. The fragility curve for each damage state is determined regarding the levels of seismic design and construction quality. The seismic design is classified into four levels of high, moderate, low, and pre-code, and the construction quality is classified into three levels of superior, ordinary and inferior.

To find that which level of fragility curves is appropriate for the vulnerability assessment of the cities with a construction quality like Sarpol-e Zahab, we studied all the possible combinations of the construction quality and seismic design levels. As shown in the second columns of Tables (5) and (6), two levels of inferior and ordinary were considered for the construction quality.

Changes in the level of seismic design were considered to be consistent with the year of publication of the various editions of the Iranian code of practice for seismic-resistant design of buildings (Standard No. 2800 of Iran). Before the year 1990, the level of seismic design was assumed pre-code. This assumption is almost consistent with the publication date of the first edition of the standard No. 2800. Between the years 1990-1999, two levels of low and moderate were considered for the buildings. The second edition of the Standard No. 2800 was published in 1999. Between the years 1999-2005, and after 2014, respectively consistent with the third and fourth editions of the Standard No. 2800, we considered two levels of the moderate and high for the seismic design levels of buildings as shown in Tables (5) and (6).

Considering two levels for each of the seismic building code at different time periods and the construction quality, as shown in Tables (5) and (6), four modes should be considered based on the HAZUS

Figure 6. Distribution of the construction age within the database.

methodology. Since the mode 4 is exactly the same as mode 1, three modes remain to be considered.

It should be mentioned that the area of the surveyed buildings constructed in the years between 2005 and 2014 constitutes 83% of the total area of the collected data, as shown in Figure (6). Therefore, the analytical damage scenario is strongly affected by the seismic design level during this period, considered to be moderate and high. In this period, the quality of the construction was considered to be one of the ordinary and inferior modes. On the contrary, for the years prior to 2005 and after 2014, changing the level of the seismic building code or the level of the construction quality, due to the low percentage of buildings built in this years, does not change much in the results.

The results of the analytical damage scenario according to HAZUS Earthquake Model must be considered as the average damage for a group of similar buildings [1]. This study compares the average value obtained from theoretical modeling with the real observed damage of the similar building types in various neighborhoods. For this purpose, three modes of fragility curves, shown in Tables (5) and (6), were considered to find out the best analytical damage scenario that is most consistent with the collected data.

Figure (7) and Table (7) provide the comparison of the analytical and the observed damage scenario of the C1M building type for the three modes of fragility curves. The information in Figure (7) and Table (7) are presented in terms of the area and the number of damaged buildings, respectively. In the procedure of the damage prediction, the intensity of the earthquake at the geo units was calculated based on the six mentioned GMPEs. According to the results, it can be concluded that none of the fragility curves alone can predict the actual results well. For example, with the Akkar and Bommer [21] relationship, using the fragility curve of mode 1, mode 2 and mode 3 leads to the moderate damage area prediction of 2282, 1455 and 3230 (m^2), respectively. However, based on the collected data, the area of 2760 m2 for moderate damage is observed. Therefore, to achieve realistic results with the least possible error, it is inevitable to use the weighted average of the three modes of fragility curves.

Considering the presented results for the CIM building type, and also the results of other building types not presented here for the sake of brevity, it can be concluded that three attenuation relationships of Boore et al. [22-25], Campbel and Bozorgnia [26], and Akkar and Bommer [21] lead approximately to the better damage scenario predictions than the others. It can also be observed the low precision prediction for the results of the Abrahamson and Silva [27] GMPE. This conclusion is consistent with the results of comparing the predicted spectral accelerations using the GMPEs and those of the recorded data presented in Table (4). Therefore, the GMPEs proposed by Boore et al. [22-25] and Campbel and Bozorgnia [26]

Table 7. Comparing the number of observed damaged building (C1M type) with those obtained from the analytical method using the various fragility curves of modes 1, 2 and 3.

		Mode 1				Mode 2				Mode 3			
		S	M	E	C	S	M	E	C	S	M	E	C
	Observation	3	11	9	1	3	11	9	1	3	11	9	1
GMPEs	Akkar and Bommer [21]	2	10	9	4	1	6	9	8	4	13	5	1
	Boore et al. [22-25]	2	9	9	4	1	6	9	8	4	13	6	1
	Campbel and Bozorgnia [26]	2	10	8	3	1	6	9	8	5	14	5	1
	Abrahamnson and Silva [27]	13	10	1	0	10	10	3	1	16	8	0	0
	Chiou and Young [28]	7	12	4	1	4	10	7	3	11	11	1	0
	Boore and Atkinson [29]	9	12	3	1	6	10	5	2	14	9	1	0

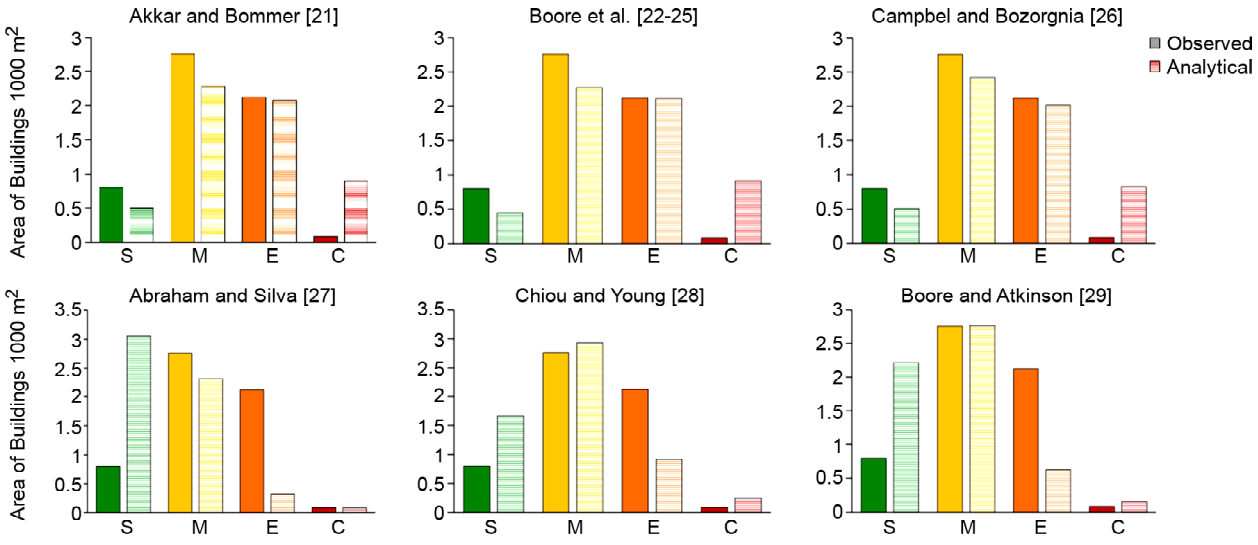

(a) Using the Fragility Curves of Mode 1

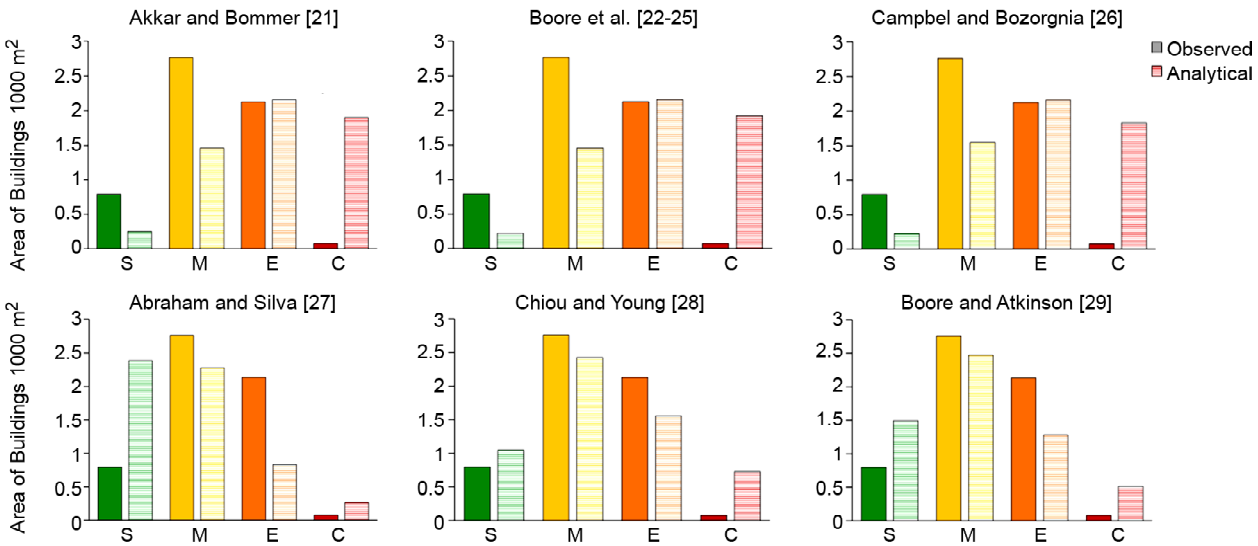

(b) Using the Fragility Curves of Mode 2

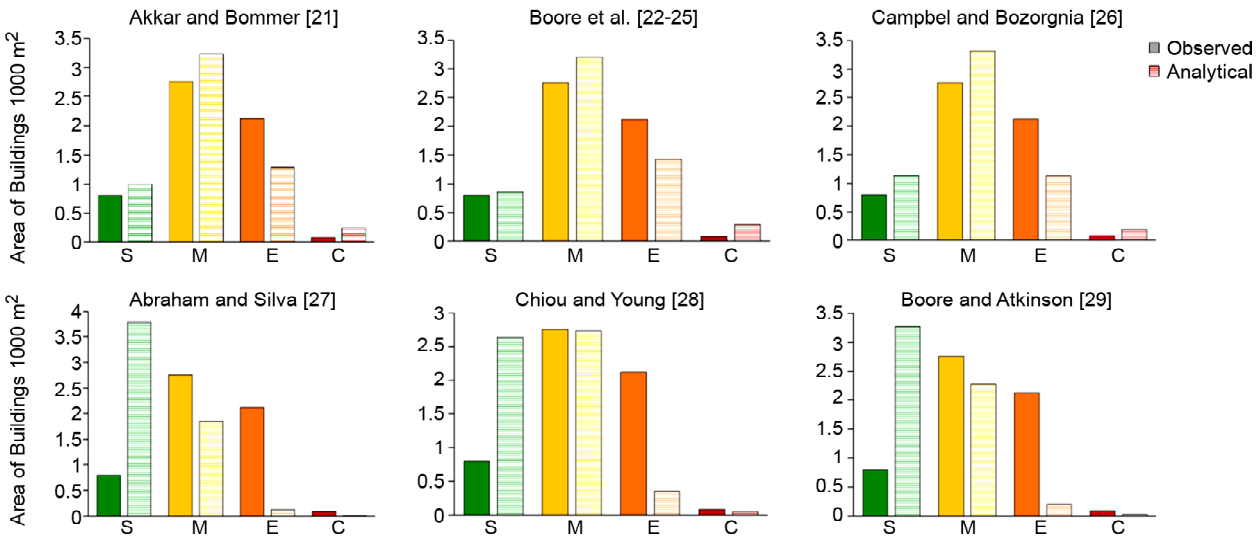

(c) Using the Fragility Curves of Mode 3

Figure 7. Comparing the observed and analytical damage scenario for C1M building type using different attenuation relationships.

in the logic tree method were used for earthquake intensity predictions at the geo units in this study. The relationship of Akkar and Bommer was not used because of the similarity of its results with those of Boore et al. [22-25] and Campbel and Bozorgnia [26].

8. Fragility Curves for Building Frames Systems

Considering all potential weighted average of fragility curves, we calculated the root mean square error (RMS error) of the four damage states to find the best combination that gives the least error. Results show that for low and mid-rise buildings with the lateral load resistance system of concrete moment frame or steel braced frame, the best fragility curve is the weighted average of fragility curves of mode 1, mode 2 and mode 3 with the weights of 0.45, 0.10 and 0.45, respectively. For buildings with steel moment frame, weights of 0.0, 0.10 and 0.90 are the most suitable. In all of these cases, the weights 0.5 and 0.5 are the best for attenuation relationships of Boore et al. [22-25] and Campbel and Bozorgnia [26], respectively.

The weighted average fragility curves for all building types can be presented in the conventional format as follows:

$$P\left(Exceedance_i \mid IM\right)=\Phi\left[\frac{1}{(\beta_{tot})_i} ln\left(\frac{IM}{LS_i}\right)\right] \quad (1)$$

where $P(.)$ is the probability of exceeding the limit state of i given the intensity measure, IM. $\Phi[.]$ is the standard normal cumulative distribution function, LS_i is the threshold value for the i^{th} limit state, and $(\beta_{tot})_i$ is the standard deviation of the logarithm of spectral displacement that represents the randomness and uncertainty components of variability.

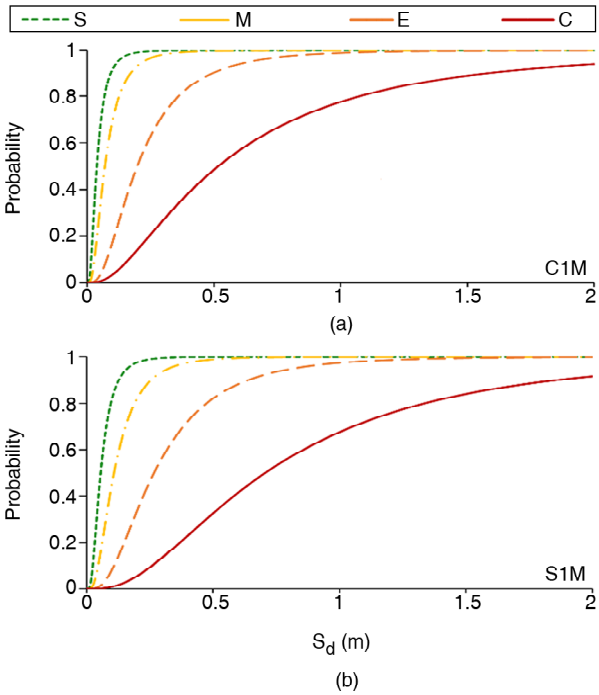

Figure 8. Developed fragility curves for various damage states and building types of C1M and S1M in Sarpol-e Zahab.

Since it is not considered practical to separate uncertainty from randomness, the combined random variable term, β_{tot}, is used to develop a composite "best estimate" fragility curve. The values of LS_i and $(\beta_{tot})_i$ for building frame systems with various height are provided as the parameters of mean and β in Table (8). To illustrate graphically, for example, Figure (8) shows the proposed fragility curves for mid-rise concrete and steel moment frame buildings in the Sarpol-e Zahab city.

9. Fragility Curves for Unreinforced Masonry Buildings

According to the different modes presented in Tables (5) and (6), the fragility curve of the desired buildings should be determined with respect to the

Table 8. Structural Fragility Curve parameters proposed for seven building types (in m).

	Slight		Moderate		Extensive		Complete	
Building Type	**Mean**	**β**	**Mean**	**β**	**Mean**	**β**	**Mean**	**β**
C1L	0.023	0.860	0.042	0.888	0.120	0.898	0.376	0.981
C1M	0.038	0.690	0.072	0.710	0.320	0.922	0.710	1.020
S1L	0.033	0.797	0.065	0.770	0.208	0.828	0.879	1.110
S1M	0.055	0.654	0.133	0.771	0.496	0.973	1.350	1.109
S2L	0.027	0.880	0.500	0.910	0.140	0.930	0.430	0.990
S2M	0.046	0.688	0.086	0.707	0.403	0.927	0.846	1.016
URML-P	0.010	0.990	0.060	0.700	0.110	0.750	0.180	0.750
URML-L	0.010	1.150	0.050	1.190	0.070	1.200	0.100	1.180
URML-M	0.005	0.900	0.008	0.950	0.010	1.000	0.046	1.050

year of construction at each mode. Considering the construction year, 27.8% of the surveyed masonry buildings (URML) were constructed before 1991, 8.7% between 1991 and 2005, and 63.5% after 2005. Thus, for example in the third mode, three fragility curves should be assigned to the URML buildings with respect to their construction year (i.e. URML-P, URML-M and URML-H where P, M, and H mean Pre, Moderate and High, respectively). The HAZUS methodology does not provide the fragility curve at the high and moderate code levels for the masonry building type. In the first and second modes, we only need the pre-code and low fragility curves that can be determined from HAZUS. For the third mode in Table (5), we studied the possibility of using the fragility relationships proposed by Frankie et al. [30] at the high and moderate code levels.

We considered all potential weighted average of mode 1, mode 2 and mode 3 for the masonry building. No weights were found that can be used to predict the observed damage scenario in all neighborhoods of the city with the acceptable accuracy. However, results show that using the weights of 0.35, 0.05 and 0.60 for mode 1, mode 2 and mode 3 of the fragility curves can predict the overall damage of the masonry buildings at the city.

The above conclusion arises for two reasons. First, we used the inappropriate fragility curves for the levels of pre-, low-, moderate-, and high-code in this type of building. Second, the classification of the quality of the construction in terms of the construction year is not appropriate for unreinforced masonry buildings. Therefore, we classified the masonry building based on the field observation according to the quality of construction. For this purpose, three categories of pre-, low-, and moderate-code were used shown with URML-P, URML-L, and URML-M, respectively.

Pre-code masonry buildings represent the buildings that have bearing stone walls with a thickness of 40 centimeters constructed with lime mortar. The ties were made using the polished gravel and plain bar. Over 40-year-old masonry buildings in the Shahrak-e Zerae Ghareblagh neighborhood collapsed during the earthquake were categorized in this group.

Low-code masonry buildings represent the buildings poorly constructed using the low-quality materials of brick, sand and cement mortar. Concrete used in ties has fine-grained and there is no connection between the vertical and horizontal ties in most cases. Moderate-code masonry buildings represent the high quality constructed buildings with bearing walls of high-quality brick, sand and cement mortar.

The mean and the standard deviation of the fragility curves for the above-mentioned pre-, low-, and moderate-code masonry buildings are provided in Table (8). These parameters were determined in a way that the theoretical model can predict the damage close to the real observed damage scenario in various neighborhoods.

10. Comparing the Theoretical and Observed Damage Scenarios

To clarify the ability of proposed fragility curves in vulnerability seismic risk assessment, we provide a comparison between the distribution of overall physical damage predicted by the analytical method and observation in Figure (9). It is clear that there

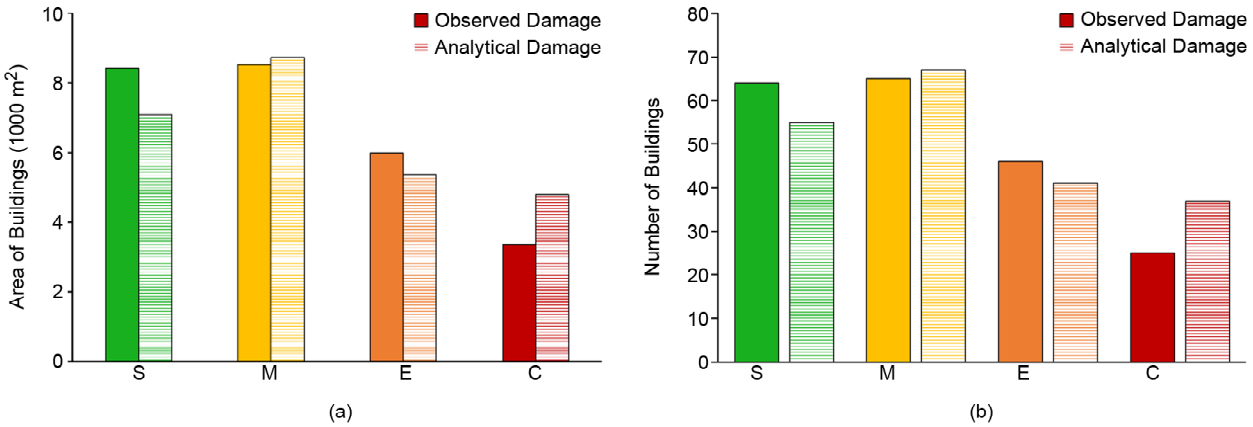

Figure 9. Comparison of the damage distribution predicted by the analytical method with the observed scenario in terms of (a) the area of buildings, and (b) the number of buildings.

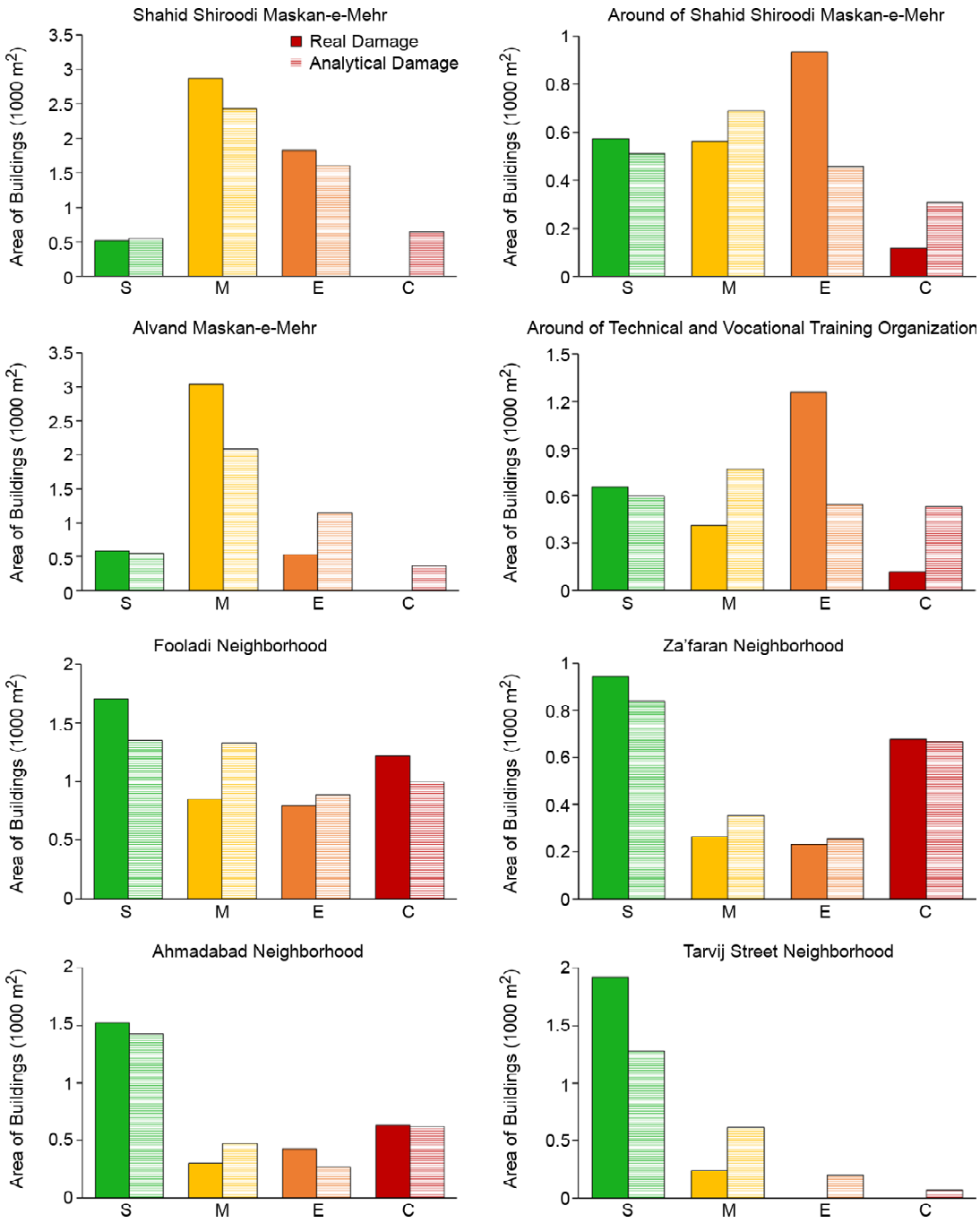

Figure 10. Comparison between the observed damage scenario in each neighborhood with the analytical damage scenario resulting from proposed fragility curves and weighted average attenuation relationship.

is a very good match in each of the damage states between the actual and analytical results in terms of the area and the number of buildings. In addition to the overall damage in the city, the amount of damage was calculated in each damage state for each geo unit and compared with the observed damage scenario. As shown in Figure (10) and Table (9), a relatively good fit is observed in terms of the area and the number of damaged buildings in all neighborhoods in the Sarpol-e Zahab city.

11. Conclusions

The focus of this study was to propose the most suitable fragility curves for different building types for the city of Sarpol-e Zahab. For this purpose, we compared the observed damage scenario in 200 buildings in various neighborhoods of the Sarpol-e Zahab city during the earthquake of November 12, 2017 with those of the analytical scenario. The earthquake intensity at the geo units was determined using the six ground motion prediction equations

Table 9. Comparison of the number of observed damaged buildings in each neighborhood with those obtained from the analytical method using the proposed fragility curves.

	Neighborhoods	Damage States			
		S	M	E	C
Observation	Shahid Shiroodi Maskan-e-Mehr	2	11	7	0
	Around the Shahid Shiroodi Maskan-e-Mehr	5	5	8	1
	Aalvand Maskan-e-Mehr	4	23	4	0
	Around the Technical and Vocational Training Organization	6	4	11	1
	Fooladi	13	7	6	10
	Za'faran	8	2	2	6
	Ahmadabad	19	4	5	8
	Tarvij Street	12	2	0	0
	Shahrak-e-Zerae Ghareblagh	0	0	0	6
Theoretical	Shahid Shiroodi Maskan-e-Mehr	2	9	6	2
	Around the Shahid Shiroodi Maskan-e-Mehr	5	6	4	3
	Aalvand Maskan-e-Mehr	4	16	9	3
	Around the Technical and Vocational Training Organization	5	7	5	5
	Fooladi	11	10	7	8
	Za'faran	8	3	2	6
	Ahmadabad	18	6	3	8
	Tarvij Street	8	4	1	0
	Shahrak-e-Zerae Gharcblagh	0	0	2	6

proposed by the Iranian guidelines for seismic hazard analysis.

The observed damage scenario was calculated by collecting the required data for each building and identifying its damage state based on the HAZUS methodology.

The attenuation relationships proposed by Boore et al. [22-25] and Campbell and Bozorgnia [26], can predict the real data at the Sarpol-e Zahab station with the minimum error regarding other considered GMPEs. Results also demonstrate that using the average of these GMPEs is the best combination to be used in the seismic vulnerability assessment of the Sarpol-e Zahab city. This combination of the GMPEs can predict the observed damage scenario with minimum RMS error with respect to other combinations considered here.

The best fragility curve for low and mid-rise buildings with the lateral load resistance system of concrete moment frame or steel braced frame is the weighted averaged of the HAZUS fragility curves at the high, moderate and low level with the weights of 0.45, 0.45 and 0.1, respectively.

The best fragility curve for steel moment frame buildings is the weighted averaged of the HAZUS fragility curves at the high, moderate and low level with the weights of 0.9, 0.0 and 0.1, respectively.

For unreinforced masonry buildings, no weighted average of the HAZUS fragility curves found that can be used to predict the observed damage scenario in all neighborhoods of the city with the acceptable accuracy. According to the observed damage scenario in the Sarpol-e Zahab city, we provide the mean and the standard deviation of the fragility curves parameters for pre-, low-, and moderate-code masonry buildings.

Damage scenario obtained from the analytical method using the proposed fragility curves have a good correspondence with the observed damage scenario of all building types at the various neighborhoods of the Sarpol-e Zahab city.

References

1. Kumar, S.A., Rajaram, C., Mishra, S., Kumar, R.P., and Karnath, A. (2017) Rapid visual screening of different housing typologies in Himachal Pradesh, India. *Natural Hazards*, **85**(3), 1851-1875.

2. Del Gaudio, C., De Martino, G., Di Ludovico, M., Manfredi, G., Prota, A., Ricci, P., and Verderame, G.M. (2017) Empirical fragility curves from damage data on RC buildings after the 2009 L'Aquila earthquake. *Bulletin of Earthquake Engineering*, **15**(4), 1425-1450.

3. Del Gaudio, C., Ricci, P., Verderame, G.M., and

Manfredi, G. (2016) Observed and predicted earthquake damage scenarios: the case study of Pettino (L'Aquila) after the 6th April 2009 event. *Bulletin of Earthquake Engineering*, **14**(10), 2643-2678.

4. Toma-Danila, D. and Armas, I. (2017) Insights into the possible seismic damage of residential buildings in Bucharest, Romania, at neighborhood resolution. *Bulletin of Earthquake Engineering*, **15**(3), 1161-1184.

5. Tavakoli, B. and Tavakoli, S. (1993) Estimating the vulnerability and loss functions of residential buildings. *Nat. Hazards*, **7**, 155-171.

6. Japan International Cooperation Agency (2000) The study on seismic micro zoning of the greater Tehran area in the Islamic Republic of Iran. *Final Report to the Government of the Islamic Republic of Iran*, Tokyo, Japan.

7. Mostafaei, H. and Kabeyasawa, T. (2003) Investigation and analysis of damage to buildings during the 2003 Bam earthquake. *B. Earthq. Res. I.*, **79**, 107-132.

8. Bakhshi, A. and Karimi, K. (2006) Method of developing fragility curves-a case study for seismic assessment of masonry buildings in Iran. *Proceedings of the 7th International Conference on Civil Engineering*, Tarbiat Modares University, Tehran, Iran.

9. Jalalian, M. (2006) *Deriving of Empirical Vulnerability Functions for Iran*. M.Sc. Thesis, Sharif University of Technology, Tehran, Iran.

10. Kazemi, H., Ghafory-Ashtiany, M., and Azarbakht, A. (2013) Effect of epsilon-based record selection on fragility curves of typical irregular steel frames with concrete shear walls in Mashhad city. *Int. J. Adv. Struct. Eng.*, **5**, 1-11.

11. Dare-Zereshki, M., Gafory-Ashtiany, M., and Mansori, B. (2008) *Developing Fragility Curves for Unreinforced Masonry Buildings of Tehran via Simplified Non-Linear Static Analysis*. M.Sc. Thesis, International Institute of Earthquake Engineering and Seismology (IIEES), Tehran, Iran.

12. Sadeghi, M., Ghafory-Ashtiany, M., and Pakdel-Lahiji, N. (2015) Developing seismic vulnerability curves for typical Iranian buildings. *Proceedings of the Institution of Mechanical Engineers, Part O: Journal of Risk and Reliability*, **229**(6), 627-640.

13. Kazemi, H., Ghafory-Ashtiany, M., and Azarbakht, A. (2017) Development of fragility curves by incorporating new spectral shape indicators and a weighted damage index: case study of steel braced frames in the city of Mashhad, Iran. *Earthquake Engineering and Engineering Vibration*, **16**(2), 383-395.

14. Methodology, M.H.L.E. (2003) *Technical Manual*. Washington, DC: Federal Emergency Management Agency (FEMA).

15. Erdik, M. et al. (2014) 'Rapid earthquake loss assessment after damaging earthquakes'. In: *Perspectives on European Earthquake Engineering and seismology, Ansal A. (ed)*, **1**. Doi: 10.1007/978-3-319-07118-3, 53-96.

16. Molina, S., Lang, D.H., Lindholm, C.D., and Lingvall, F. (2010) *User Manual for the Earthquake Loss Estimation Tool: SELENA*. http://selena.sourceforge.net. Accessed 29 Nov. 2015.

17. Molina, S., Lang, D.H., and Lindholm, C.D. (2010) SELENA-An open-source tool for seismic risk and loss assessment using a logic tree computation procedure. *Computers and Geosciences*, **36**(3), 257-269.

18. Erdik, M., Sesetyan, K., Demircioglu, M.B., Tüzün, C., Giardini, D., Gulen, L., Akkar, D., and Zare, M. (2012) Assessment of seismic hazard in the middle east and caucasus: EMME (earthquake model of middle east) project. *Proceedings of the 15th World Conference on Earthquake Engineering*. Lisbon, Portugal.

19. IIEES (2017) *Report of Sarpol-e Zahab Earthquake of 12 November 2017*. International Institute of Earthquake Engineering and Seismology, Iran.

20. Department of Technical Affairs (2014) *Guide-*

line for Seismic Hazard Analysis. Vice Presidency for Strategic Planning and Supervision, Iran.

21. Akkar, S. and Bommer, J.J. (2010) Empirical equations for the prediction of PGA, PGV and spectral accelerations in europe, the Mediterranean region and the middle east. *Seismological Research Letters*, **81**(2), 195-206.

22. Boore, D.M., Joyner, W.B., and Fumal, T.E. (1993) *Estimation of Response Spectra and Peak Accelerations from Western North American Earthquakes: An Interim Report*. Open-File Report 93-509. U.S. Geological Survey, 70p.

23. Boore, D.M., Joyner, W.B., and Fumal, T.E. (1994) *Estimation of Response Spectra and Peak Accelerations from Western North American Earthquakes: An Interim Report*. Part 2. Open-File Report 94-127. U.S. Geological Survey.

24. Boore, D.M., Joyner, W.B., and Fumal, T.E. (1997a) Equations for estimating horizontal response spectra and peak acceleration from western North American earthquakes: A summary of recent work. *Seismological Research Letters*, **68**(1), 128-153.

25. Boore, D.M., Joyner, W.B., and Fumal, T.E. (1997b) *Estimation of Response Spectra and Peak Accelerations from Western North American Earthquakes: An Interim Report*. Technical report, U.S. Geological Survey. Open-File Report 94-127.

26. Campbell, K. and Bozorgnia, Y. (2008) NGA ground motion model for the geometric mean horizontal component of PGA, PGV, PGD and 5%-damped linear elastic response spectra for periods ranging from 0.01 to 10 s. *Earthquake Spectra*, **24**(1), 139-171.

27. Abrahamson, N. and Silva, W. (2008) Summary of the abrahamson and silva NGA ground motion relations. *Earthquake Spectra*, **24**(1), 67-97.

28. Chiou, B.S. and Young, R.R (2008) An NGA model for the average horizontal component of peak ground motion and response spectra. *Earthquake Spectra*, **24**(1), 173- 215.

29. Boore, D. and Atkinson, G. (2008) Ground motion prediction equations for the average horizontal component of PGA, PGV, and 5%-damped PSA at spectral periods between 0.01 s and 10.0 s. *Earthquake Spectra*, **24**(1), 99-138.

30. Frankie, T.M., Gencturk, B., and Elnashai, A.S. (2012) Simulation-based fragility relationships for unreinforced masonry buildings. *Journal of Structural Engineering*, **139**(3), 400-410.